Characteristics of solar proton events associated with ground level enhancements

S. Y. Oh,[1] Y. Yi,[2] J. W. Bieber,[1] P. Evenson,[1] and Y. K. Kim[3]

Received 7 December 2009; revised 16 June 2010; accepted 21 June 2010; published 15 October 2010.

[1] In certain explosive events, the Sun emits large numbers of protons with energy up to tens of GeV. Particle acceleration processes on the Sun can be understood through the observation of such energetic particles. According to the definition of NOAA Space Environment Services Center, a solar proton event (SPE) is defined as an event with a peak intensity of >10 pfu (particle flux unit; 1 particle cm^{-2} sr^{-1} s^{-1}) for >10 MeV protons. Major SPEs are not always associated with ground level enhancements (GLEs), whereas relatively minor SPEs are sometimes associated with GLEs. We examined the peak intensities of 85 SPEs after 1986 using the intensity of proton differential energy channels (P3–P10) from GOES. We identified 31 SPEs associated with GLEs having well-defined profiles with a large increase and clear peak for each proton channel. They have larger peak intensity and fluence and shorter delay time between onset and peak than SPEs without GLEs. Fluences and peak intensities of SPEs have a good correlation with percent increases of GLEs, with the best correlation coefficients obtained for the peak intensities and fluences of channels P8, P9, and P10. For these energy channels (spanning 350–700 MeV), we find that there are threshold values for GOES fluence and peak intensity such that most SPEs above the threshold are associated with GLEs, whereas almost none below the thresholds are.

Citation: Oh, S. Y., Y. Yi, J. W. Bieber, P. Evenson, and Y. K. Kim (2010), Characteristics of solar proton events associated with ground level enhancements, *J. Geophys. Res.*, *115*, A10107, doi:10.1029/2009JA015171.

1. Introduction

[2] Solar proton events (SPEs) occur when protons are accelerated to very high energies either close to the Sun during a solar flare or by Coronal Mass Ejection (CME)-driven shocks in the corona or in interplanetary space. More generally, one can speak of solar energetic particle (SEP) events, but since our study is in fact based on observations of the proton component, we adopt the more restrictive terminology. An SPE is said to occur if there is an increase >10 pfu (particle flux unit; 1 particle cm^{-2} sr^{-1} s^{-1}) in the flux of >10 MeV protons (http://umbra.nascom.nasa.gov/SEP). This definition has been applied for many studies of SPEs. Some events are also recorded as ground level enhancements (GLEs), first identified by *Forbush* [1946], when sudden increases in cosmic ray intensity are observed by ground-based detectors, at present generally neutron monitors. GLEs are clearly related to SPEs, but questions remain regarding the exact nature of the relationship. As detailed below, major SPEs sometimes occur without an associated GLE, whereas conversely some minor SPEs are accompanied by GLEs.

[3] *El-Borie* [2003] examined 58 extremely large SPEs (with a flux of over 10 pfu at energy ≥60 MeV) between January 1973 and May 2001. Nearly 40% of these events were associated with GLEs. The profile of flux as a function of time showed multiple particle injection or varying particle acceleration either at the solar source or in propagation to the Earth. He also found that large GLEs did not necessarily come from a sequence of major proton events and were not a condition for observing major solar proton fluxes. In another study, *Cliver* [2006] addressed that although the SPE is a favorable condition for GLE occurrence, it is not a requirement. It does not contradict El Borie's results.

[4] *Kurt et al.* [2004] made a catalog of 253 SPEs with energy of >10 MeV and peak intensity of >10 pfu at the Earth's orbit for three complete 11-year solar cycles (1970–2002). The catalog lists SPE properties (onset time, peak flux), associated Hα flare properties (time of start and maximum, position, importance, active region), and GLE association. They described the association with other events using a correlation analysis. From this set of 253 events, 231 can be identified with Hα flares and 42 registered as GLEs. The longitudinal distribution of the associated flares shows that most SPEs are connected with western hemisphere flares. The correlation coefficients are 0.53 with soft X-ray (SXR) flares, 0.73 with sunspot number, 0.71 with solar flare index, and 0.86 with coronal index. These correlations are likely manifestations of the "big flare syndrome" [*Kahler*, 1982].

[5] *Wang* [2006] made a statistical study of 163 SPEs associated with X-ray flares, CME, and radio type II bursts

[1]Department of Physics and Astronomy and Bartol Research Institute, University of Delaware, Newark, Delaware, USA.
[2]Department of Astronomy and Space Science, Chungnam National University, Daejeon, South Korea.
[3]Department of Nuclear Engineering, Hanyang University, Seoul, South Korea.

0148-0227/10/2009JA015171

during January 1997–June 2005. He classified events by the peak flux of >10 MeV solar protons into three groups (large: >100 pfu, moderate: 10–100 pfu, minor: 1–10 pfu). Using the >10 MeV proton channel, *Wang* [2006] concluded that the most intense SPEs are likely to be produced by major flares located near the central meridian of the Sun with shock waves driven by very fast halo CME ($v \geq 1600$ km/s). He suggested that CME-driven shock acceleration is a necessary condition for large proton production.

[6] *Kuwabara et al.* [2006] developed a system that detects count rate increases recorded in real time by eight neutron monitors and triggers an alarm if a GLE is detected. The GLE alert precedes the earliest indication from GOES (100 MeV or 10 MeV protons) by ~10–30 minutes. *Kuwabara et al.* [2006] listed proton events associated with GLE, classifying them in terms of intensity of >10 MeV (moderate radiation storm: S2, strong: S3, extreme: S4). They showed that the maximum intensity of protons does not have a particularly good correlation with whether the event produces a GLE.

[7] In contrast to the work with integral intensity, differential proton energy channels on GOES are used in some studies of SPE. *Reames and Ng* [1998] used the intensities of proton energy channels (P3, P5, P7) on GOES 6 to explore the streaming limit imposed by wave-particle interactions. *Lario et al.* [2008] used the intensities of proton energy channels (P5, P7) on GOES to explain events exceeding the streaming limit.

[8] *Tylka et al.* [2006] explored whether the difference between GLEs and exceptionally large SPEs is primarily spectral in nature. Speculation on the physical cause of these spectral differences appears in *Tylka et al.* [2005] and *Tylka and Lee* [2006]. *Tylka and Dietrich* [2009] noted the excellent correlation between GOES High Energy Proton and Alpha Detector fluences and neutron monitor fluences.

[9] In summary, most previous studies of SPEs considered only integral intensity, with the conclusion that the peak intensity of SPE has a poor correlation with GLE and that major SPEs are not a necessary condition for GLEs. On the other hand, minor SPEs are sometimes associated with GLEs. In this paper, we explore the possibility that association with a GLE depends not on the integral intensity of particles, but on some other aspect of their energy spectrum. We present the results of a statistical study of SPE and GLE focusing on the higher proton energy channels (P3 and above) on GOES.

2. Data and Method

[10] We based our study primarily on the SPE list from NOAA Space Environment Services Center (SESC) (http://umbra.nascom.nasa.gov/SEP), which identifies 225 SPEs from 1976 to 2006 on the basis of 5-minute averages of the integral proton flux above an energy level of 10 MeV, given in pfu, measured by GOES spacecraft at geosynchronous orbit. SESC defines the start of a proton event to be the first of three consecutive data points with fluxes greater than or equal to 10 pfu. The end of an event is the last time the flux was greater than or equal to 10 pfu. We also referred to the SPE list made by *Kurt et al.* [2004], which broke apart the multiple events coming in quick succession from a single listing in the NOAA list. We added eight more events to the NOAA SESC list.

[11] From the initial 233 SPEs, our available database was reduced to 178 SPEs occurring during 1986–2006 because GOES data are available only from 1986 onward and the SPE list maintained by SESC extends only to 2006. From these events, we selected 85 SPEs that display a clear solar proton signal in GOES channels P6 and P7, of which 31 are associated with GLEs. Eight of the SPEs fall within data gaps for high-energy channels (P8–P11), of which a disproportionate number (five) are associated with GLEs. Consequently, as discussed below, we constructed a simple proxy using IMP 8 data (Charged Particle Measurement Experiment; http://data.ftecs.com/archive/imp_cpme/) for use in part of our analysis. Because the accuracy of the P11 integral flux has been questioned [*Smart and Shea*, 1999], we generally omit the P11 differential flux from the figures and from our narrative. For completeness, we do include the P11 channel in some of the tables, however.

[12] Table 1 lists the 85 SPEs. The first column is simply a sequence number we have assigned to specify the event, with a superscript *a* to indicate the events for which no data exist for P8–P11. We then show the onset date (year and month), start time of P6, peak time of P6, peak intensity of P6, the generally accepted GLE number for events associated with GLE, and finally the GOES spacecraft (6, 7, 8, 10 or 11) used for that particular event.

[13] For each SPE, we determined the peak intensity, the fluence for the half day following the peak, and the delay time between onset and peak. If there is an associated GLE in the list from the Oulu neutron monitor station (http://cosmicrays.oulu.fi/GLE.html), we also recorded its percentage increase and the delay time between the GLE and SPE. We also studied the correlation between the peak GLE intensity and the peak of each proton channel. We note that the use of a single station to characterize the GLE peak introduces possible distortions from anisotropy of the solar particle distribution. In spite of this, we document below significant correlations between the Oulu peak and GOES energy channels; possibly these correlations would be even stronger if anisotropy were taken into account.

[14] If SPEs have fluctuating profiles or statistical noise, it is difficult to determine a clear peak. Choosing the largest fluctuation as the peak is essentially meaningless. This can be particularly true of the higher-energy channels. If there is no clear peak in channels P8–P10, we make a 1-hour average around the peak of the P7 profile. In the following, we shorten "SPE associated with GLE" to "SPE with GLE" and "SPE not associated with GLE" to "SPE without GLE". The term fluence (*counts* cm^{-2} sr^{-1} MeV^{-1}) as used in this paper is the time-integrated intensity during the half day interval beginning at the peak computed from 5-minute average intensity (*counts* cm^{-2} sec^{-1} sr^{-1} MeV^{-1}). We prefer the definition of fluence to the fluence integrated over the whole event, because event onset is often difficult to define, especially in minor events, and because the half-day limitation avoids energetic storm particle (ESP) increases associated with the shock's arrival at 1 AU.

3. Results

[15] Figure 1 shows examples of the time profile of SPE for integral intensities of >10 MeV. The SPE of April 15, 2001, is shown in Figure 1a and that of September 13, 2004,

Table 1. List of 85 Solar Proton Events

SPE Number	Onset Date		Start of P6 (dd:hh:mm)	Peak of P6 (dd:hh:mm)	P6 Peak Intensity (cm^{-2} sr^{-1} s^{-1} MeV^{-1})	GLE Number	GOES Data
	Year	Month					
1	1986	Feb.	06:08:15	06:12:30	2.480E−2		06
2	1986	Feb.	07:13:05	07:17:20	3.280E−2		06
3	1986	Feb.	14:10:10	14:12:20	2.290E−2		06
4	1986	May	04:12:15	04:13:25	4.680E−3		06
5	1988	Mar.	25:21:55	25:22:15	8.630E−3		07
6	1988	Nov.	08:13:20	08:16:30	6.150E−3		07
7	1988	Nov.	13:23:40	14:00:15	3.240E−3		07
8	1988	Dec.	14:13:15	14:21:15	7.010E−3		07
9	1988	Dec.	16:09:50	16:15:15	8.730E−3		07
10	1989	Mar.	23:20:05	23:20:25	4.890E−3		07
11	1989	Jun.	18:15:25	18:16:30	9.840E−3		07
12	1989	Jul.	25:08:50	25:10:30	5.310E−2	40	07
13	1989	Aug.	12:22:50	13:04:30	5.450E−1		07
14	1989	Aug.	16:01:15	16:04:00	4.600E−1	41	07
15	1989	Sep.	29:11:45	29:15:55	2.630E+0	42	07
16	1989	Oct.	19:13:00	19:20:20	1.650E+0	43	07
17	1989	Oct.	22:17:50	22:19:05	1.810E+0	44	07
18	1989	Oct.	24:18:20	24:22:40	9.480E−1	45	07
19	1989	Nov.	15:07:10	15:08:15	3.030E−2	46	07
20	1989	Nov.	30:21:35	31:00:35	1.700E−2		07
21[a]	1990	May	21:22:35	22:03:10	1.870E−1	47	07
22[a]	1990	May	24:21:05	25:00:30	1.770E−1	48	07
23[a]	1990	May	26:21:00	27:00:55	1.260E−1	49	07
24[a]	1990	May	28:05:15	28:10:45	4.060E−2	50	07
25	1990	Jul.	25:23:45	26:04:50	4.230E−3		07
26	1991	Mar.	23:17:05	24:03:50	1.440E+0		07
27	1991	May	13:02:05	13:03:40	6.190E−2		07
28	1991	Jun.	11:02:25	11:10:15	5.870E−1	51	07
29	1991	Jun.	15:08:30	15:10:00	6.310E−1	52	07
30	1991	Oct.	30:06:55	30:08:05	2.930E−2		07
31	1992	Jun.	25:20:15	25:21:00	1.380E−1	53	07
32[a]	1992	Oct.	30:18:30	30:23:05	1.520E−1		07
33[a]	1992	Nov.	02:03:10	02:05:40	1.100E+0	54	07
34[a]	1993	Mar.	04:12:40	04:13:30	7.010E−3		07
35[a]	1993	Mar.	12:18:40	12:19:45	2.120E−2		07
36	1994	Feb.	20:01:45	20:02:25	4.980E−3		07
37	1994	Oct.	19:21:40	19:23:30	4.270E−3		07
38	1997	Nov.	04:06:35	04:07:45	2.470E−2		08
39	1997	Nov.	06:12:25	06:15:25	4.500E−1	55	08
40	1998	Apr.	21:08:30	21:11:05	7.740E−2		08
41	1998	May	02:13:55	02:14:25	9.290E−2	56	08
42	1998	May	06:08:15	06:08:40	4.880E−2	57	08
43	1998	Aug.	24:22:35	25:00:30	3.590E−2	58	08
44	1998	Sep.	30:14:05	30:16:05	3.090E−2		08
45	1998	Nov.	14:07:40	14:08:50	6.110E−2		08
46	1999	Jun.	01:20:45	02:01:10	6.580E−3		08
47	2000	Feb.	18:09:40	18:09:55	4.230E−3		08
48	2000	Jun.	10:17:20	10:17:55	1.590E−2		08
49	2000	Jul.	14:10:30	14:12:00	4.160E+0	59	08
50	2000	Jul.	22:12:00	22:12:20	3.680E−3		08
51	2000	Sep.	12:13:25	12:21:30	4.400E−3		08
52	2000	Oct.	16:07:10	16:09:25	3.280E−3		08
53	2000	Nov.	08:23:30	09:03:40	3.650E+0		08
54	2000	Nov.	24:15:30	24:17:10	1.200E−2		08
55	2001	Jan.	28:16:45	28:17:45	2.970E−3		08
56	2001	Apr.	02:22:55	03:03:50	5.460E−2		08
57	2001	Apr.	10:07:20	10:12:40	5.160E−3		08
58	2001	Apr.	15:13:50	15:15:05	1.390E+0	60	08
59	2001	Apr.	18:02:40	18:03:55	1.210E−1	61	08
60	2001	Jun.	15:16:00	15:16:45	3.250E−3		08
61	2001	Aug.	16:00:30	16:02:55	3.040E−1		08
62	2001	Sep.	24:14:10	24:23:05	3.290E−1		08
63	2001	Oct.	19:02:15	19:02:55	2.630E−3		08
64	2001	Oct.	22:15:40	22:19:20	8.690E−3		08
65	2001	Nov.	04:16:35	04:17:30	5.560E−1	62	08
66	2001	Nov.	22:22:45	23:07:25	4.410E−2		08
67	2001	Dec.	26:05:45	26:07:00	4.880E−1	63	08
68	2002	Apr.	21:01:35	21:04:15	2.460E−1		08
69	2002	Aug.	22:02:45	22:04:15	1.650E−2		08
70	2002	Aug.	24:01:15	24:02:15	2.880E−1	64	08

Table 1. (continued)

SPE Number	Onset Date Year	Onset Date Month	Start of P6 (dd:hh:mm)	Peak of P6 (dd:hh:mm)	P6 Peak Intensity (cm^{-2} sr^{-1} s^{-1} MeV^{-1})	GLE Number	GOES Data
71	2003	May	31:02:40	31:03:30	8.630E−3		08
72	2003	Oct.	26:17:50	26:18:15	1.110E−2		10
73	2003	Oct.	28:11:10	28:16:00	2.140E+0	65	10
74	2003	Oct.	29:20:40	29:22:30	1.070E+0	66	10
75	2003	Nov.	02:17:25	02:18:20	5.160E−1	67	10
76	2003	Nov.	04:20:00	05:02:10	1.160E−2		10
77	2004	Nov.	01:06:05	01:06:50	1.560E−2		11
78	2004	Nov.	07:17:30	07:20:45	5.810E−3		11
79	2005	Jan.	17:12:30	17:14:25	3.080E−1	68	11
80	2005	Jan.	20:06:40	20:07:05	6.460E+0	69	11
81	2005	Jun.	16:20:50	16:22:05	2.870E−2		11
82	2005	Aug.	22:22:10	23:01:00	3.620E−3		11
83	2005	Sep.	08:16:35	08:18:10	7.450E−2		11
84	2006	Dec.	07:05:05	07:12:00	1.880E−1		11
85	2006	Dec.	13:02:45	13:04:35	8.630E−1	70	11

[a]The event has no data of P8–P11 channels.

in Figure 1b. The former SPE occurs with a GLE, and the latter without a GLE. There is no apparent difference between these profiles other than a factor of 3 difference in intensity level. In contrast, the time profiles of the differential channels P3–P10 have major differences for these same events as shown as Figures 2 and 3. Indeed, the SPE without GLE is nearly undetectable in these higher-energy (>∼100 MeV) channels.

[16] In Figure 2, the SPE with GLE exhibits well-defined profiles with large increases and clear peaks for each proton energy channel. The SPE without GLE in Figure 3 has uncertain profiles lacking clear peaks for channels P6 and higher, with a time structure dominated by statistical noise for each proton energy channel. By examining the time profiles of proton energy channels for 85 SPEs, we found this behavior characteristic, namely, that SPEs with GLEs have well-defined profiles through all channels. Increase of intensity in high-energy protons of SPEs is closely related to the association with a GLE. The >10 MeV integral intensity of a SPE cannot predict an association with a GLE, but the differential intensity of high-energy protons is related closely with the GLE.

[17] Figure 4 illustrates this systematic trend throughout our sample of events as a series of plots for different energy channels of the SPE peak intensity as a function of event number. The association with a GLE depends on the intensities of higher-energy proton channels.

[18] Figure 5 is similar to Figure 4, except that it shows the fluence (half day following peak) for each proton energy channel. As with the peak intensity, there exist large differences of fluence between SPEs with and without GLEs.

[19] Table 2 gives the average (both mean and median) peak intensity for each proton energy channel. Of 85 SPEs, 31 are associated with GLEs. The mean peak intensity of SPEs with GLEs is larger relative to that of SPEs without GLEs, as the proton energy increases. Although the mean intensity of SPEs with GLEs is influenced by a few large events, the median intensity shows the same trend. The difference is more than a factor of 10. The mean peak intensities of P8, P9, and P10 have especially clear differences as is also apparent in Figure 4. We note that for each GOES differential channel, we report the peak intensity in the first 12 hours of the event [*Cliver and Ling*, 2007] to avoid the ESP increases associated with shock arrival.

[20] Table 3 shows that the mean fluence during the half-day interval beginning at the peak for each proton energy channel displays essentially the same distribution as mean peak intensity. Mean and median fluences of SPEs with GLEs have a difference of about a factor of 10 compared to SPEs without GLEs. The basic conclusion is that only SPEs with high, long-lasting intensity of high-energy protons (P8 and above) are recorded as GLEs.

[21] Table 4 reports the delay time between onset and peak of SPEs for the P3–P7 channels. As the energy of proton channels gets higher, delay time between onset and peak gets shorter. Mean delay time between onset and peak is 2.74 ± 0.26 hours for P6 and 2.64 ± 0.26 hours for the P7 channel. Mean and median delay times for SPEs with GLEs are both shorter than those of SPEs without GLEs. For the P6 channel, mean delay time of SPEs with GLEs is 2.49 ± 0.35 hours and that of SPEs without GLEs is 2.98 ± 0.35 hours. For P7 channel, that of SPEs with GLEs is 2.37 ± 0.37 hours and that of SPEs without GLEs is 2.87 ± 0.37 hours. The onset-peak delay times for SPEs with GLEs are shorter than that for SPEs without GLEs on the order of ~20–30 minutes on average, for protons above 80 MeV. But the differences are of marginal statistical significance due to the small data set.

[22] Table 5 shows the delay time between the GLE peak and the SPE peak. Most GLEs precede the associated SPEs. As the energy of proton channel gets higher, the delay time gets shorter. This is almost certainly due to velocity dispersion.

[23] Figure 6 shows the correlation between the peak intensity of SPEs and percentage increase of GLEs for each proton energy channel. All 31 events were used for P3–P7, but only 26 events were available for the channels P8–P10. A similar analysis of the fluence is shown in Figure 7. Linear and logarithmic correlation coefficients for P3–P11 channels are given in Table 6. Peak intensities of P8–P10 show the highest coefficients among the proton energy channels tested. This indicates that the higher-energy GOES

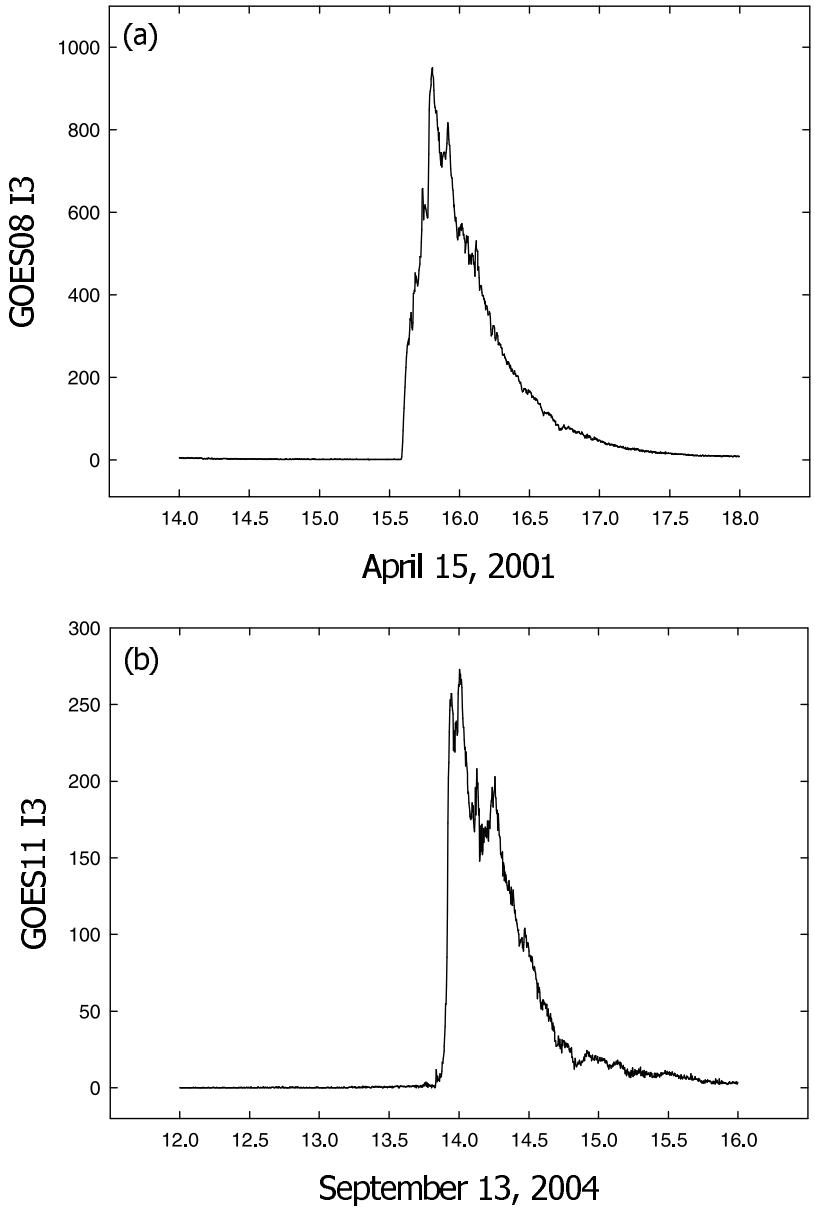

Figure 1. Time profiles of integral GOES proton fluxes >10 MeV. (a) April 15, 2001, SPE with GLE. (b) September 13, 2004, SPE without GLE. The difference in integral intensity between these two events is a factor of 3.

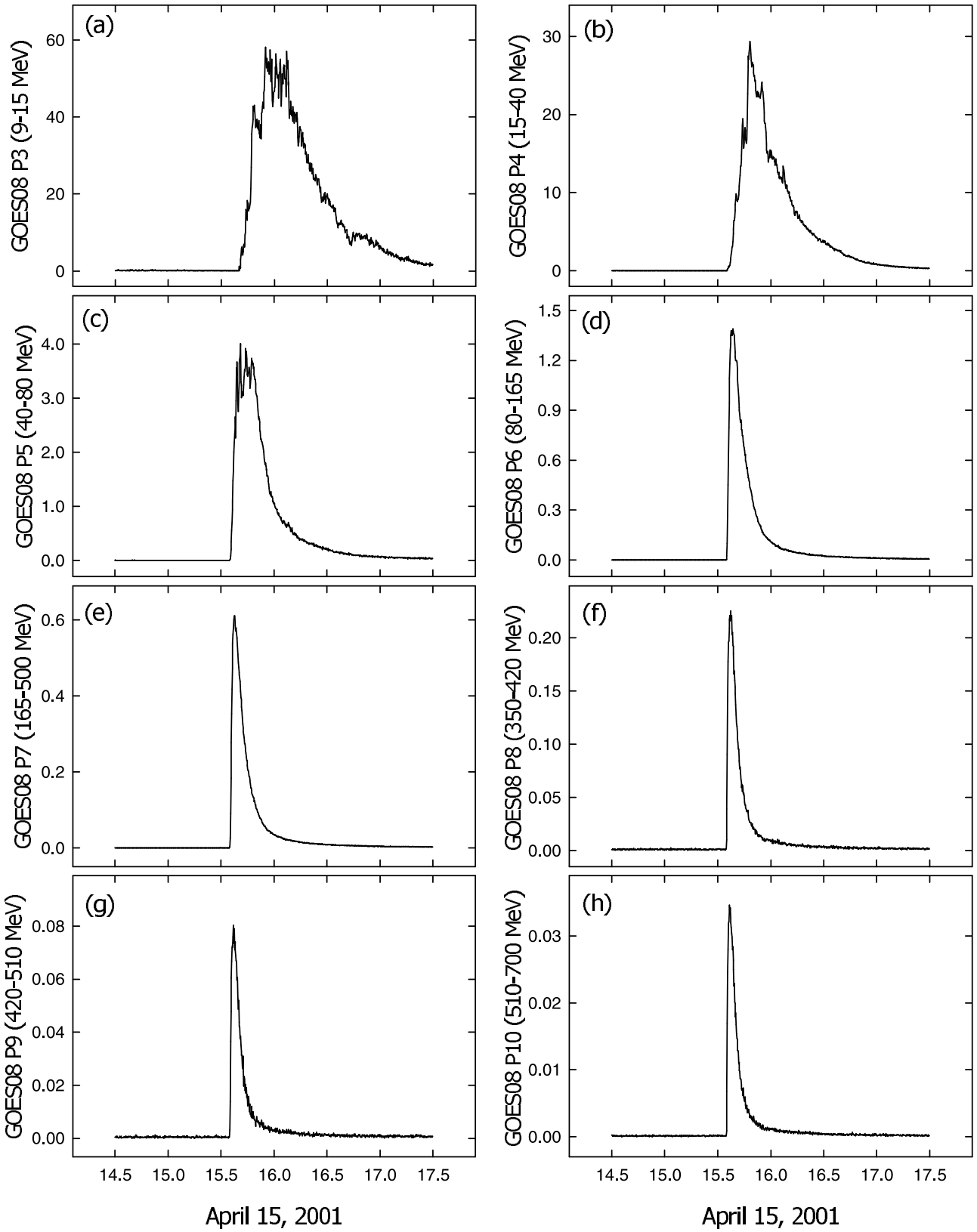

Figure 2. Time profile of various high-energy differential GOES proton channels for the SPE with GLE of April 15, 2001. (a) P3, (b) P4, (c) P5, (d) P6, (e) P7, (f) P8, (g) P9, (h) P10.

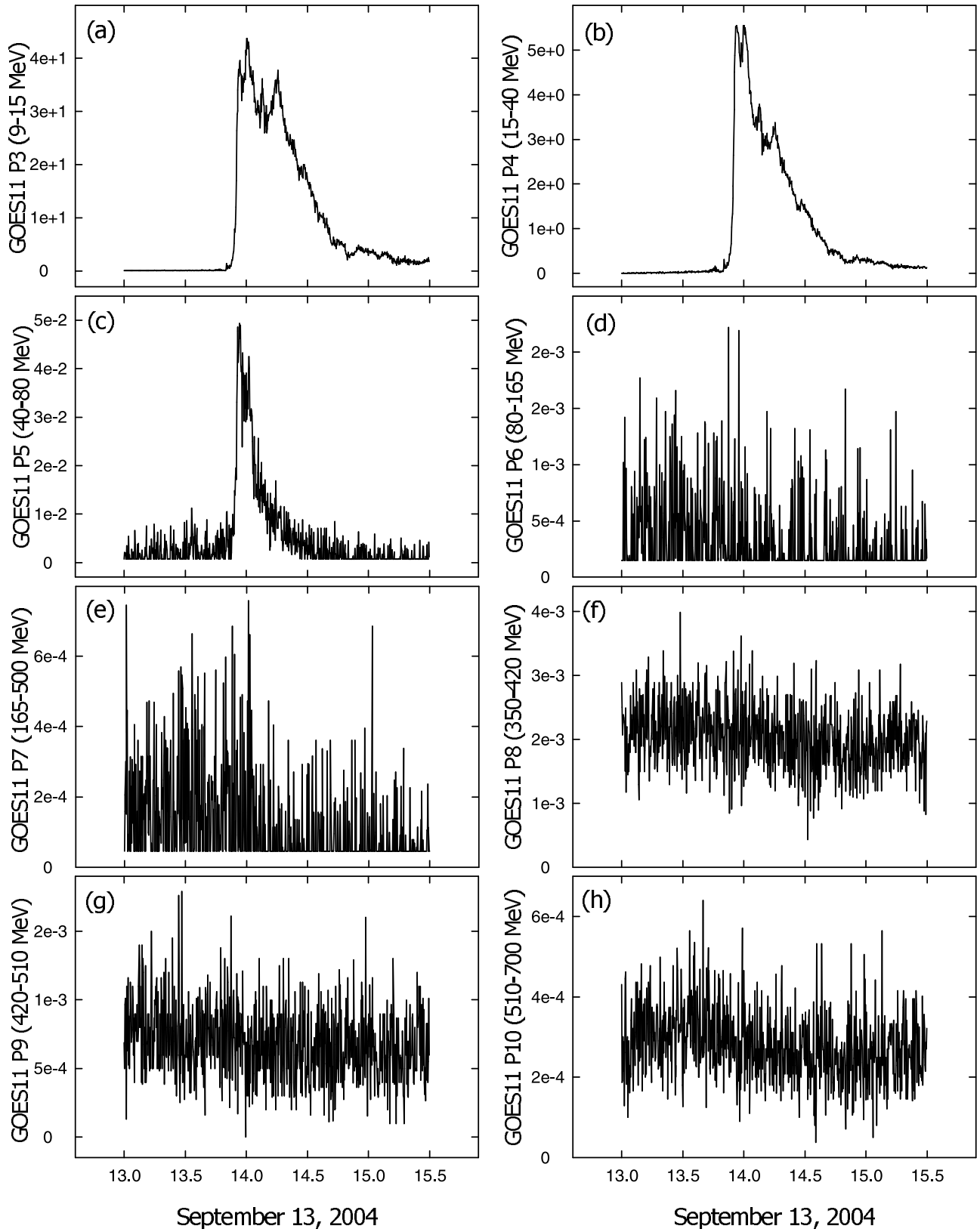

Figure 3. Same as Figure 2 except for the SPE without GLE of September 13, 2004.

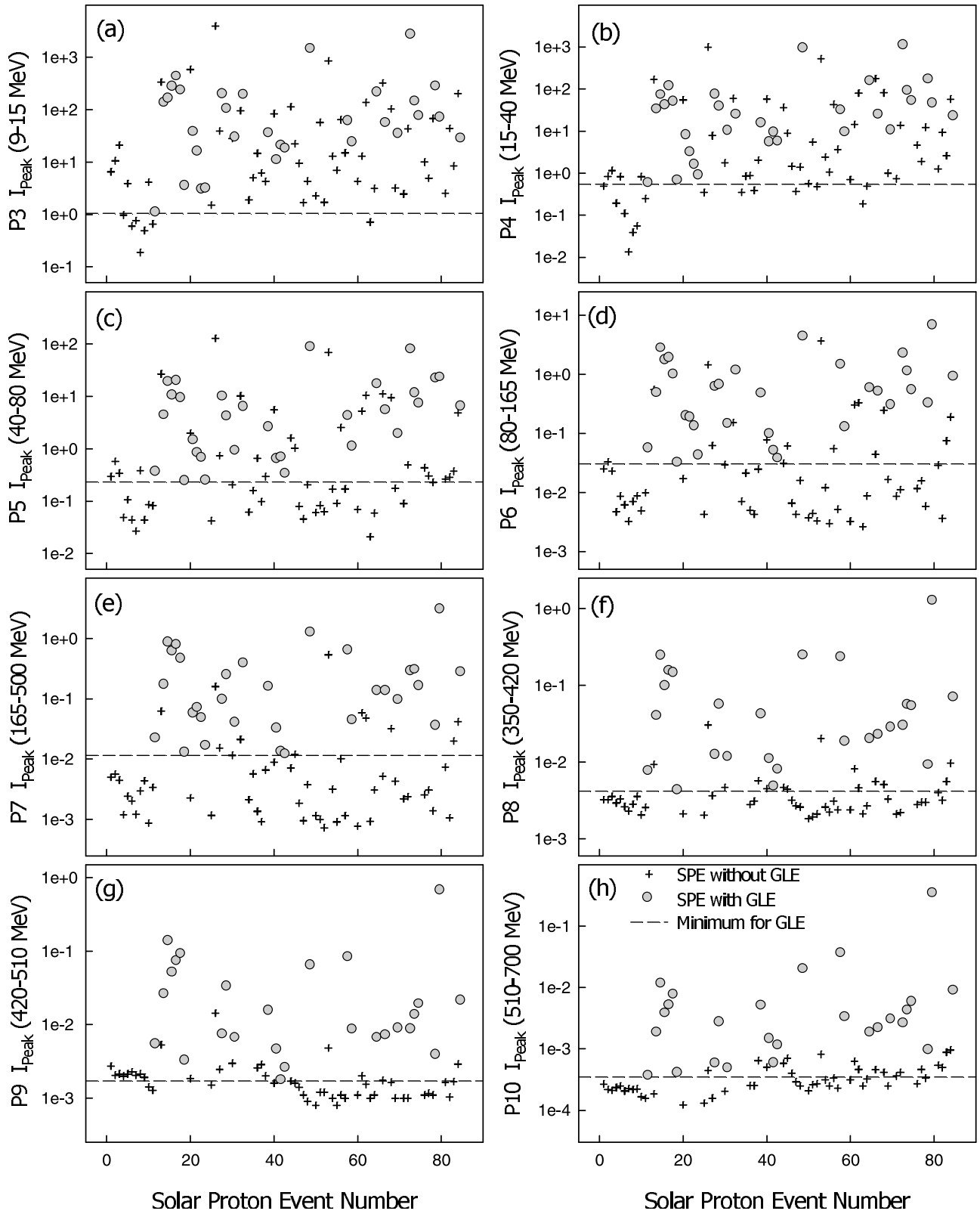

Figure 4. Peak intensity (I_{Peak}) for proton channels P3–P10. The arrangement of the images corresponds to that of Figures 2 and 3. Crosses indicate SPEs without GLEs, and circles indicate SPEs with GLEs. The dashed horizontal lines show the minimum peak intensity of SPE with GLE for each energy channel.

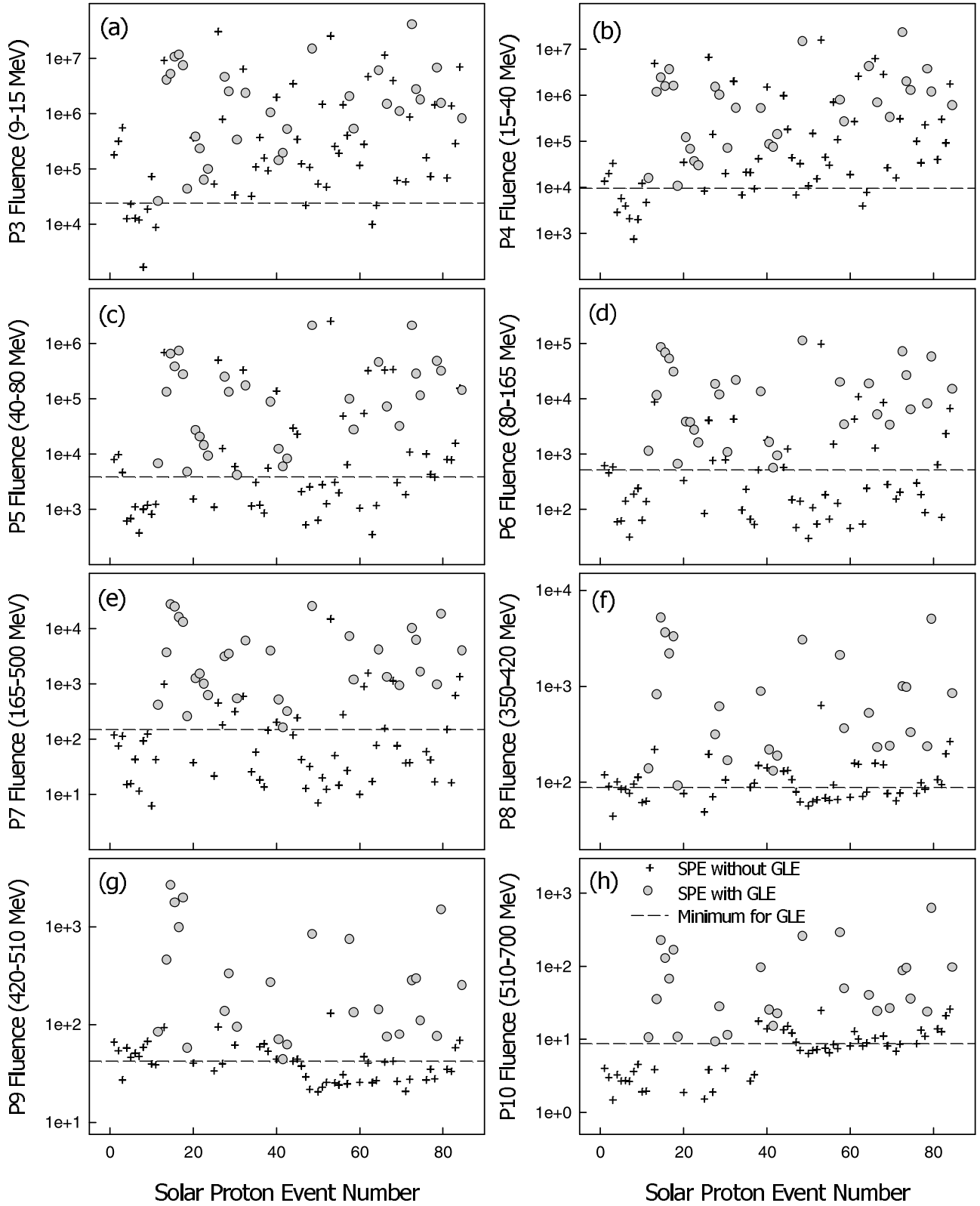

Figure 5. Similar to Figure 4, except that fluence that the half day beginning at the peak is plotted.

Table 2. Average Peak Intensity (cm^{-2} sr^{-1} s^{-1} MeV^{-1}) for Proton Energy Channels P3–P11

	Without GLE	With GLE	All
Proton Channel	54[a] (51[b])	31[a] (26[b])	85[a] (77[b])
P3 (9–15 MeV)	1.356E+2 (8.905E+0)	2.170E+2 (5.810E+1)	1.653E+2 (2.100E+1)
P4 (15–40 MeV)	4.508E+1 (1.415E+0)	9.555E+1 (2.320E+1)	6.349E+1 (5.470E+0)
P5 (40–80 MeV)	5.475E+0 (2.455E−1)	1.101E+1 (4.150E+0)	7.492E+0 (6.080E−1)
P6 (80–165 MeV)	1.422E−1 (1.180E−2)	9.534E−1 (4.880E−1)	4.381E−1 (4.060E−2)
P7 (165–500 MeV)	2.120E−2 (3.125E−3)	3.247E−1 (1.290E−1)	1.319E−1 (1.150E−2)
P8 (350–420 MeV)	3.204E−3 (1.720E−3)	1.073E−1 (3.375E−2)	3.836E−2 (2.354E−3)
P9 (420–510 MeV)	1.211E−3 (5.644E−4)	5.112E−2 (1.089E−2)	1.806E−2 (8.277E−4)
P10 (510–700 MeV)	2.171E−4 (1.511E−4)	1.754E−2 (2.760E−3)	6.067E−3 (2.040E−4)
P11 (>700 MeV)	1.557E−4 (1.445E−4)	4.591E−3 (4.890E−4)	1.653E−3 (1.896E−4)

[a]Total number of SPE.
[b]Number of SPE with data for channels P8–P11. Entries: Mean (Median).

Table 3. Average Fluence (the half day interval beginning at the peak; cm^{-2} sr^{-1} MeV^{-1}) for Proton Energy Channels P3–P11[a]

Proton Channel	Without GLE	With GLE	All
P3 (9–15 MeV)	2.168E+6 (1.705E+5)	3.980E+6 (1.451E+6)	2.829E+6 (3.577E+5)
P4 (15–40 MeV)	9.028E+5 (3.378E+4)	2.009E+6 (6.328E+5)	1.306E+6 (1.005E+5)
P5 (40–80 MeV)	1.047E+5 (3.449E+3)	2.758E+5 (1.059E+5)	1.671E+5 (9.740E+3)
P6 (80–165 MeV)	3.025E+3 (2.171E+2)	2.040E+4 (1.071E+4)	9.361E+3 (7.659E+2)
P7 (165–500 MeV)	4.746E+2 (5.411E+1)	5.680E+3 (2.866E+3)	2.373E+3 (2.010E+2)
P8 (350–420 MeV)	1.127E+2 (8.871E+1)	1.208E+3 (5.453E+2)	4.826E+2 (1.197E+2)
P9 (420–510 MeV)	4.353E+1 (3.975E+1)	4.967E+2 (1.876E+2)	1.965E+2 (5.312E+1)
P10 (510–700 MeV)	8.218E+0 (7.501E+0)	9.042E+1 (3.593E+1)	3.597E+1 (9.118E+0)
P11 (>700 MeV)	5.825E+0 (5.078E+0)	3.287E+1 (1.056E+1)	1.496E+1 (6.699E+0)

[a]Format as in Table 2.

Table 4. Average Delay Time Between SPE Onset and SPE Peak[a]

	Without GLE			With GLE			All		
Proton Channel	Mean (hour)	Median (hour)	Error ($\sigma_1/\sqrt{N_1}$)	Mean (hour)	Median (hour)	Error ($\sigma_2/\sqrt{N_2}$)	Mean (hour)	Median (hour)	Error ($\sigma/\sqrt{N}$)
P3 (9–15 MeV)	4.75	3.83	0.3992	3.94	3.25	0.5064	4.45	3.83	0.3148
P4 (15–40 MeV)	4.26	3.63	0.4036	4.19	3.75	0.5283	4.23	3.67	0.3188
P5 (40–80 MeV)	3.67	2.54	0.3970	3.31	2.75	0.4072	3.54	2.58	0.2918
P6 (80–165 MeV)	2.98	2.08	0.3532	2.49	1.83	0.3523	2.74	1.83	0.2584
P7 (165–500 MeV)	2.87	1.92	0.3657	2.37	1.50	0.3451	2.64	1.58	0.2642

[a]σ, σ_1, σ_2: standard deviation of all SPE, SPE without GLE, and SPE with GLE. N, N_1, N_2: event number of all SPE (85), SPE without SPE (54), and SPE with GLE (31).

Table 5. Delay Time Between the GLE Peak and the SPE Peak

Proton Channel	Mean (hour)	Median (hour)
P6 (80–165 MeV)	1.71	1.25
P7 (165–500 MeV)	1.53	1.00
P8 (350–420 MeV)	0.99	0.75
P9 (420–510 MeV)	0.84	0.58
P10 (510–700 MeV)	0.79	0.50
P11 (>700 MeV)	0.70	0.38

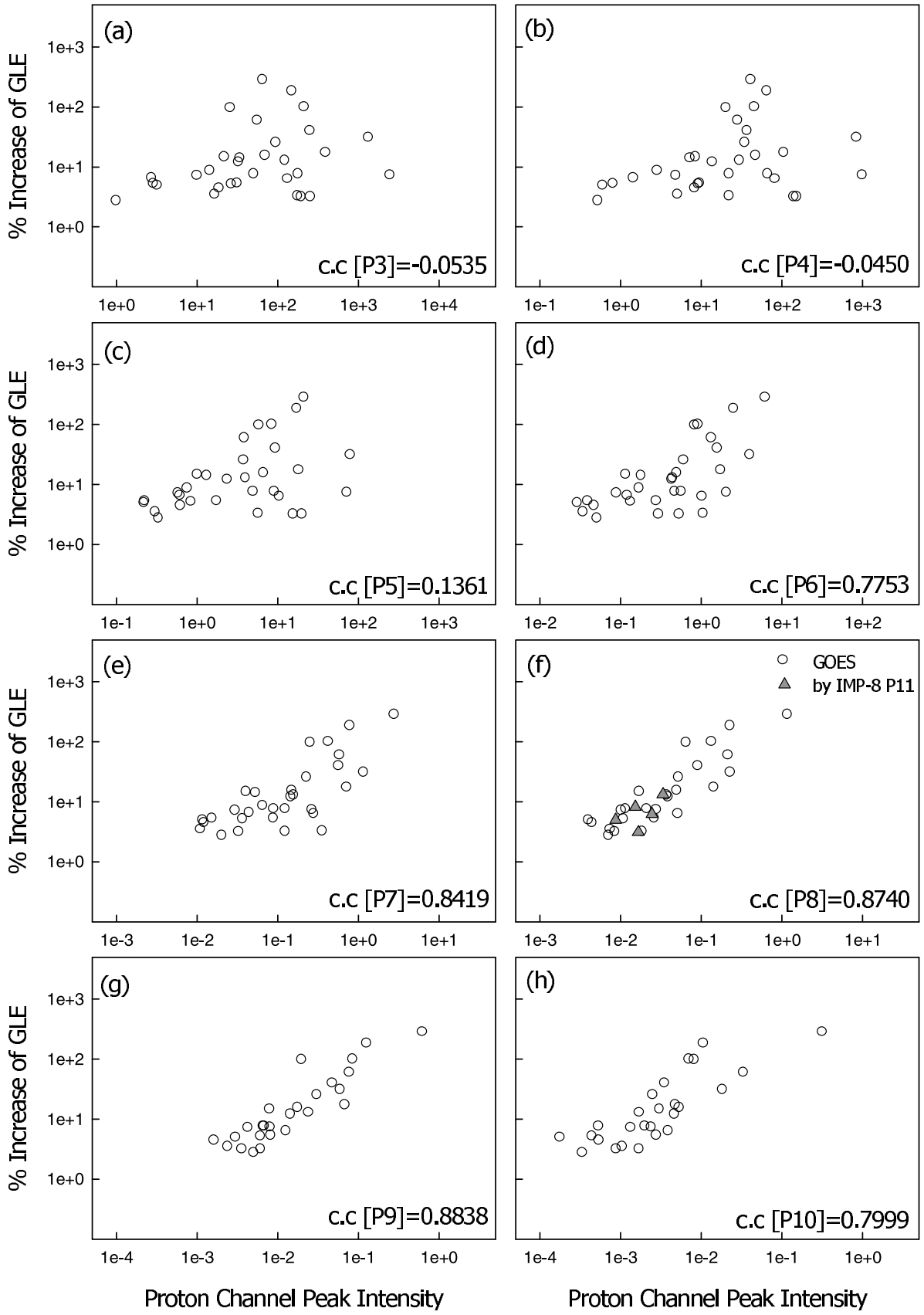

Figure 6. Correlation between peak intensity of SPE and percentage increase of GLE for each proton energy channel. The images are arranged as in Figures 2 through 5. Linear correlation coefficients are also given. Filled triangle in (f) shows the intensity estimated by IMP 8 P11.

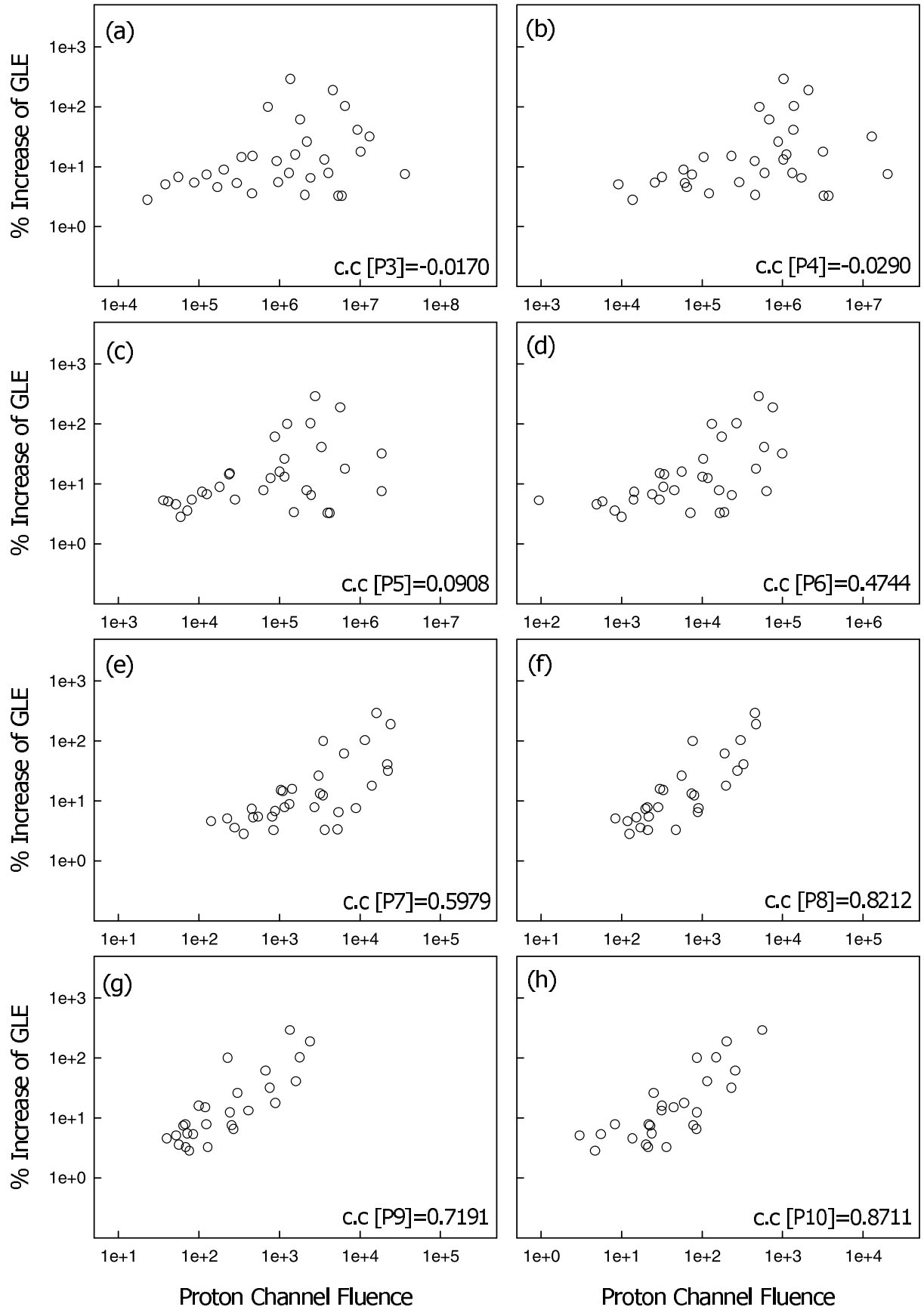

Figure 7. Correlation between fluence of SPE and percentage increase of GLE for each proton energy channel as in Figure 6.

Table 6. Correlation Coefficients Between Peak Intensity/Fluence of SPE and Percent Increase of GLE

Proton Channel	Peak Intensity		Fluence	
	Linear	Logarithmic	Linear	Logarithmic
P3 (9–15 MeV)	−0.0535	0.3001	−0.0170	0.3602
P4 (15–40 MeV)	−0.0450	0.3213	−0.0290	0.3730
P5 (40–80 MeV)	0.1361	0.4429	0.0908	0.4519
P6 (80–165 MeV)	0.7753	0.6625	0.4744	0.5894
P7 (165–500 MeV)	0.8419	0.7432	0.5979	0.6913
P8 (350–420 MeV)	0.8740[a]	0.8726[a]	0.8212	0.8304
P9 (420–510 MeV)	0.8838	0.8993	0.7191	0.8341
P10 (510–700 MeV)	0.7999	0.8238	0.8711	0.7886
P11 (>700 MeV)	0.8666	0.9121	0.7844	0.8512

[a]Estimated GOES P8 using the intensity of IMP-8 P11. The other high-energy proton channels are calculated using 26 events excluding 5 events with no data of P8–P11.

protons typically exhibit spectral continuity with the particles that produce the GLEs, whereas the lower-energy GOES protons do not.

[24] The correlations, particularly for the peak in P8, are excellent, but unfortunately there are no GOES data for five of the GLEs. To determine whether there might be any exceptions, we constructed a simple proxy for the GOES P8 channel (filled triangles in Figure 6f) using the peak intensity of the IMP 8 P11 channel (190–440 MeV), which overlaps the energy range of GOES P8 (350–420 MeV). A simple linear regression of the two has a correlation coefficient $R = 0.9263$. We used this regression to produce the points plotted in Figure 6f. (We could not apply the IMP 8 data in case of the fluence because of the data gaps of IMP 8 data.) Our conclusion is that the relation between approximately 400 MeV protons and GLE intensity is quite robust, which might be expected considering that GLE particles typically have a median energy of ~1–2 GeV [e.g., *Bieber et al.*, 2002, 2004].

4. Discussion

[25] We have demonstrated that there is a pronounced threshold effect for SPEs associated with GLEs, such that all events below the threshold are SPEs without GLEs, whereas the majority of events above the threshold are SPEs with GLEs. In Figure 4, this threshold was set by the event with the minimum GOES channel intensity (at the peak) that was accompanied by a GLE. For channel P6, for example, 38 of 85 SPEs were below the threshold. By construction, none of these events was accompanied by GLEs. Of 47 SPEs above the threshold, however, 66% were accompanied by GLEs. As shown in the left-hand part of Table 7, the threshold effect becomes more pronounced for channels P6–P10 as channel energy increases.

[26] A similar effect occurs if the threshold is based upon the fluence of each GOES energy channel rather than the peak. As shown in the right-hand part of Table 7, the effect is clear for GOES channels P6–P10, though less pronounced than for a threshold based upon peak intensity. The association between GLEs and SPEs above the threshold is much stronger than that between GLEs and radiation storm intensity as tabulated by *Kuwabara et al.* [2006; Table 4]. Presumably, this is because radiation storm intensity is quantified by the GOES >10 MeV integral channel, whereas our analysis is based upon GOES differential channels of energy ~100 MeV and upward.

[27] These characteristics may be related to the result of *Tylka and Dietrich* [2009], who concluded that SPE spectra from 10 MeV to 10 GeV are well represented by a "Band function" [*Band et al.*, 1993], which displays a smooth rollover from a harder power law at low energies to a softer power law at high energies. On the basis of the two events presented in their Figure 1, it appears that the low-energy power law index may not be very well correlated with the high-energy index. This is consistent with our observation that the association between GLEs and SPEs gets progressively weaker as one considers lower and lower SPE energies.

[28] The fact that the most intense SPEs, as measured in GOES channels P6 and above, tend to be associated with GLEs has potential ramifications for using neutron moni-

Table 7. Number of SPE Below/Above the Minimum Threshold of Peak Intensity and Fluence

Proton Channel	Peak Intensity				Fluence			
	Minimum Threshold	Below	Above		Minimum Threshold	Below	Above	
			Without GLE	With GLE			Without GLE	With GLE
P3 (9–15 MeV)	1.040E+0	7	47	31	2.421E+4	10	44	31
P4 (15–40 MeV)	5.460E−1	14	40	31	9.704E+3	13	41	31
P5 (40–80 MeV)	2.300E−1	27	27	31	3.847E+3	28	26	31
P6 (80–165 MeV)	3.030E−2	38	16	31	5.177E+2	35	19	31
P7 (165–500 MeV)	1.150E−2	42	12	31	1.504E+2	39	15	31
P8 (350–420 MeV)	4.160E−3	43	8	26	8.836E+1	25	26	26
P9 (420–510 MeV)	1.700E−3	43	8	26	4.213E+1	31	20	26
P10 (510–700 MeV)	3.510E−4	44	7	26	8.762E+0	33	18	26
P11 (>700 MeV)	1.940E−4	42	9	26	5.468E+0	26	25	26

tors as a space weather tool. Owing to the high speed of relativistic solar cosmic rays, an alert system based upon neutron monitor data can provide an early alert of an extreme radiation storm that is 10–30 minutes earlier than the earliest proton alert issued by the Space Weather Prediction Center [*Kuwabara et al.*, 2006]. Further, the fact that peak GLE intensity is well correlated with peak GOES channel intensity (Figure 6 and Table 6) suggests that neutron monitor observations may have predictive value for SPE differential intensity to energies at least as low as ~100 MeV. This possibility will be examined further in a forthcoming publication.

[29] Although we have referred to the events under discussion as solar proton events (SPE), this should not be taken to mean that the accelerated particles are exclusively protons. In fact, there is a strong tendency for SPEs with GLEs to be iron-rich at high energy [*Tylka et al.*, 1999; *Lopate*, 2001]. Taking account of the differing characteristics of proton- and iron-specific yield functions, *Tylka et al.* [1999] concluded that the Fe contribution to the neutron monitor signal was at most 10% during the September 29, 1989, SPE. *Lopate* [2001] concluded that energetic iron nuclei contributed no more than 9% of the count rate recorded by Climax neutron monitor during the same event.

[30] **Acknowledgments.** This work was supported by the BAERI Nuclear R&D program of the Ministry of Education, Science and Technology (MEST)/ Korea Science and Engineering Foundation (KOSEF) and by the National Research Foundation of Korea Grant funded by the Korean Government (NRF-2009-352-C00051). This work was also supported by NASA LWS grant NNX08AQ18G and by NASA/EPSCoR Cooperative Agreement NNX09AB05A. The lists of GLEs and SPEs are archived at Oulu neutron monitor station operated by Sodankyla Geophysical Observatory and at NOAA Space Environment Services Center. We thank all these data managers: Ilya Usoskin, Joe Kunches, and Joseph B. Gurman.

[31] Philippa Browning thanks Galina Bazilevskaya and another reviewer for their assistance in evaluating this paper.

References

Band, D., J. Matteson, L. Ford, B. Schaefer, D. Palmer, B. Teegarden, T. Cline, M. Briggs, W. Paciesas, G. Pendleton, G. Fishman, C. Kouveliotou, C. Meegan, R. Wilson, and P. Lestrade (1993), BATSE observations of gamma-ray burst spectra. I. Spectral diversity, *Astrophys. J.*, *413*, 281–292.

Bieber, J. W., W. Droge, P. A. Evenson, R. Pyle, D. Ruffolo, U. Pinsook, P. Tooprakai, M. Rujiwarodom, T. Khumlumlert, and S. Krucker (2002), Energetic particle observations during the 2000 July 14 solar event, *Astrophys. J.*, *567*, 622–634.

Bieber, J. W., P. Evenson, W. Droge, R. Pyle, D. Ruffolo, M. Rujiwarodom, P. Tooprakai, and T. Khumlumlert (2004), Spaceship Earth observations of the Easter 2001 solar particle event, *Astrophys. J.*, *601*, L103–L106.

Cliver, E. W. (2006), The unusual relativistic solar proton events of 1979 August 21 and 1981 May 10, *Astrophys. J.*, *639*, 1206–1217.

Cliver, E. W., and A. G. Ling (2007), Electrons and protons in solar energetic particle Events, *Astrophys. J.*, *658*, 1349–1356.

El-Borie, M. A. (2003), Major solar-energetic particle fluxes: I. Comparison with the associated ground level enhancement of cosmic rays, *Astroparticles Phys.*, *19*, 549–558.

Forbush, S. E. (1946), The first identification of solar proton events in 1942, *Phys. Rev.*, *70*, 771.

Kahler, S. W. (1982), The role of the big flare syndrome in correlations of solar energetic proton fluxes and associated microwave burst parameters, *J. Geophys. Res.*, *87*, 3439–3448, doi:10.1029/JA087iA05p03439.

Kurt, V., A. Belov, H. Mavromichalaki, and M. Gerontidou (2004), Statistical analysis of solar proton events, *Ann. Geophys.*, *22*, 2255–2271.

Kuwabara, T., J. W. Bieber, J. Clem, P. Evenson, and R. Pyle (2006), Development of a ground level enhancement alarm system based upon neutron monitors, *Space Weather*, *4*, S10001, doi:10.1029/2006SW000223.

Lario, D., A. Aran, and R. B. Decker (2008), Major solar energetic particle events of solar cycles 22 and 23: Intensities above the streaming limit, *Space Weather*, *6*, S12001, doi:10.1029/2008SW000403.

Lopate, C. (2001), Climac neutron monitor response to incident iron ions: An application to the 29 Sept 1989 ground level event, *Proc. of 27th Int. Cosmic Ray Conf.*, *8*, 3398–3400.

Reames, D. V., and C. K. Ng (1998), Streaming-limited intensities of solar energetic particles, *Astrophys. J.*, *504*, 1002–1005.

Smart, D. F., and M. A. Shea (1999), Comment on the use of GOES solar proton data and spectra in solar dose calculations, *Rad. Meas.*, *30*(3), 327–335.

Tylka, A. J., and W. F. Dietrich (2009), A new and comprehensive analysis of proton spectra in ground-level enhanced (GLE) solar particle events, *31th Int. Cosmic Ray Conf.*, SH 1.5, 273.

Tylka, A. J., and M. A. Lee (2006), A model for spectral and compositional variability at high energies in large, gradual solar particle events, *Astrophys. J.*, *646*, 1319–1334.

Tylka, A. J., W. F. Dietrich, C. Lopate, and D. V. Reames (1999), High-energy solar Fe ions in the 29 September 1989 ground level event, *Proc. of 26th Int. Cosmic Ray Conf.*, *6*, 67–70.

Tylka, A. J., C. M. S. Cohen, W. F. Dietrich, M. A. Lee, C. G. Maclennan, R. A. Mewaldt, C. K. Ng, and D. V. Reames (2005), Shock geometry, seed populations, and the origin of variable elemental composition at high energies in large gradual solar particle events, *Astrophys. J.*, *625*, 474–495.

Tylka, A. J., C. M. S. Cohen, W. F. Dietrich, M. A. Lee, C. G. Maclennan, R. A. Mewaldt, C. K. Ng, and D. V. Reames (2006), A comparative study of ion characteristics in the large gradual solar energetic particle events of 2002 April 21 and 2002 August 24, *Astrophys. J. Suppl. Ser.*, *164*, 536–551.

Wang, R. (2006), Statistical characteristics of solar energetic proton events from January 1997 to June 2005, *Astroparticles Phys.*, *26*, 202–208.

J. W. Bieber, P. Evenson, and S. Y. Oh, Department of Physics and Astronomy, University of Delaware, Newark, DE 19716, USA. (syoh@bartol.udel.edu)

Y. K. Kim, Department of Nuclear Engineering, Hanyang University, Seoul 133-791, South Korea.

Y. Yi, Department of Astronomy and Space Science, Chungnam National University, Daejeon 305-764, South Korea.